Received: 27 August 2018 | Revised: 21 November 2018 | Accepted: 29 November 2018

DOI: 10.1002/bit.26885

ARTICLE

WILEY BIOTECHNOLOGY AND BIOENGINEERING

Construction of efficient bioelectrochemical devices: Improved electricity production from cyanobacteria (*Leptolyngbia* sp.) based on π-conjugated conducting polymer/gold nanoparticle composite interfaces

Emre Cevik[1] | Mustafa Buyukharman[2] | Huseyin Bekir Yildiz[2,3]

[1]Genetic Research Department, Institute for Research & Medical Consultations (IRMC), Imam Abdulrahman Bin Faisal University, Dammam, Saudi Arabia

[2]Department of Metallurgical and Materials Engineering, KTO Karatay University, Konya, Turkey

[3]Biotechnology Research Lab, FELSIM Ltd. Inc., Konya Technocity, Konya, Turkey

Correspondence
Emre Cevik, Genetic Research Department, Institute for Research & Medical Consultations (IRMC), Imam Abdulrahman Bin Faisal University, P.O. Box: 1982, Dammam 31441, Saudi Arabia.
Email: ecevik@iau.edu.sa;
Huseyin Bekir Yildiz, Department of Metallurgical and Materials Engineering, KTO Karatay University, 42020 Konya, Turkey.
Email: huseyinbekir.yildiz@karatay.edu.tr

Abstract

In this study, gold electrodes (GE) were coated with conducting polymers to obtain a high photocurrent using cyanobacteria from a novel bioelectrochemical fuel cell. For this purpose, 4-(4H-ditiheno[3,2-b:2',3'-d]pyrol-4-yl) aniline and 5-(4H-dithieno[3,2-b:2',3'-d]pyrol-4-yl) napthtalane-1-amine monomers were coated on GE by performing an electropolymerization process. After that, gold nanoparticles (AuNP) were specifically modified by 2-mercaptoethane sulfonic acid and p-aminothiophenol to attach to the electrode surface. The conducting polymers GE coat was modified with functionalized AuNP using a cross-linker. The resulting electrode structures were characterized by cyclic voltammetry and chronoamperometry under on-off illumination using a fiber optic light source. Cyanobacteria *Leptolyngbia* sp. was added to the GE/conducting polymer/AuNP electrode surface and stabilized by using a cellulose membrane. During the illumination, water was oxidized by the photosynthesis, and oxygen was released. The released oxygen was electrocatalytically reduced at the cathode surface and a 25 nA/cm^2 photocurrent was observed in GE/*Leptolyngbia* sp. After the electrode modifications, a significant improvement in the photocurrent up to 630 nA/cm^2 was achieved.

KEYWORDS

bioelectrochemical fuel cell, conducting polymer, cyanobacteria *Leptolyngbia* sp., photocurrent, photosynthesis

1 | INTRODUCTION

Nowadays, countries have increased their efforts in the use of new, clean, and sustainable energy sources as an alternative to fossil fuels for energy needs. Therefore, the potential of renewable energy sources is expected to play an important role in global energy infrastructure in the future (Logan et al., 2006; Bullen, Arnot, Lakeman, & Walsh, 2006; Rashid, Cui, Saif Ur Rehman, & Han, 2013; Sawa et al., 2017). Unlike fossil fuels, researchers continue to find sustainable, renewable, and less polluting resources (Strik et al., 2008). Reports show that solar energy is the most important alternative energy source in nature and solar-based natural and renewable energy conversion systems stand out in terms of efficiency and sustainability (Heldt & Piechulla, 2011). Biofuel cells and bioelectrodes, which convert solar energy into electricity using natural photosynthesis, are rapidly developing and reported extensively in the literature (Bombelli et al., 2011; McCormick et al., 2011).

Photosynthesis is used by plants and bacteria to transform light energy into chemical energy. The main process is water splitting by the action of sunlight into oxygen and hydrogen in photosynthesis (Bidwell, 1957; Logan et al., 2006; Carpentier, Loranger, Chartrand, & Purcell, 1991). The sunlight is absorbed by the complex proteins photosystem I

and II (PSI and PSII) called reaction centers that are found in the thylakoid membrane in the structure. The photons emitted from the light source are absorbed by the PSII reaction center (P680 protein complex) and excited to a higher energy level. Electrons in the high energy level are captured by the plastoquinone complexes (Q_A and Q_B; electron acceptors) and transferred to another protein complex (cytochrome b6f [Cyt b_6f]) and then transferred to the PSI complex. The reaction center, known as P700, absorbs another photon to create a higher energy level electron and these electrons are carried by the electron acceptors phylloquinone and ferrodoxine (FD) to reduce $NADP^+$ to NADPH. As a result of that, ATP is formed (Çevik, Carbas, Senel, & Yildiz, 2018; Haehnel, 1977; Hasan, Çevik et al., 2015; Hernandez & Newman, 2001; Hsu, Lee, & Pan, 1986).

Among the photosynthetic organisms, cyanobacteria are widely preferred to harvest electricity (Sawa et al., 2017) from sunlight in bioelectrochemical fuel cells (BFCs) due to their high productivity, compatibility for direct electricity generation, and easy adaptation to the environment (Torimura, Miki, Wadano, Kano, & Ikeda, 2001). Besides that, unlike higher plants and algae, cyanobacteria contain photosynthetic and respiratory systems in their thylakoid membranes. For this reason, excess electrons produced during photosynthesis are transferred to the respiratory system and this does not lead to oxidative stress (Torimura et al., 2001). Moreover, at high light intensity to prevent photo-damage, they use a special mechanism and this mechanism helps them to be able to survive under different environmental conditions. Furthermore, the use of whole bacterial cells in such systems does not require any isolation process (Torimura et al., 2001). Therefore, cyanobacteria offer a practical and versatile use to generate electricity from solar energy.

BFCs are devices that are used to convert sunlight into electrical energy by using biological materials and photosynthetic reaction centers (Bullen et al., 2006; Gajda, Greenman, Melhuish, & Ieropoulos, 2013). Recently there have been a number of reported studies based on BFCs facilitated by cyanobacteria, for example, *Geobacter sulfurreducens* (Nishio, Hashimoto, & Watanabe, 2013), *Synechococcus* sp. PPC 7942 (Torimura et al., 2001), *Anabaena variabilis* (Sekar, Umasankar, & Ramasamy, 2014), *Synechocystis* sp. PCC 6803 (Bombelli et al., 2011; Torimura et al., 2001), *Rhodobacter Capsulatus* (Hasan, Reddy et al., 2015), *Shewanella oneidensis* (Gorby et al., 2006), and mostly using the redox mediator to transfer extracellular electrons to the electrode. To facilitate the electron transfer (ET) various electrode materials, such as carbon felt, graphite, carbon brush, various types of platinum (Pt), gold (Au), and indium-tin-oxide (ITO) have been used in BFC studies (Bullen et al., 2006). Reports demonstrated that direct electricity generation and long-term stability feature of cyanobacteria lead to practical use in BFC systems to generate electricity.

Conducting polymers have been reported in many studies (Dervisevic, Çevik, Şenel, Nergiz, & Abasiyanik, 2016; Khan et al., 2008; Nergiz, Dervisevic, Çevik, 2013; Şenel, Bozgeyik, Çevik, & Fatih Abasıyanık, 2011; Şenel, Çevik, & Abasıyanık, 2010; Soylemez et al., 2015; Vidal, Garcia, & Castillo, 2002) with features such as easy synthesis, wide application range, good environmental stability, and long-lasting electrical conductivity. In the field of continuously growing conductive polymers, the synthesis and application of conductive polymers with π-conjugated systems have attracted huge interest in recent years (Rahman, Kumar, Park, & Shim, 2008). These polymers exhibit very good optical and electronic properties (Udum et al., 2014), low cost synthesis, ability to be used in flexible large devices, and ability to combine with inorganic semiconductors (Wang, Dong, Hu, Liu, & Zhu, 2012). According to recent reports, conductive polymers with dithienopyrrole (DTP) have attracted researchers' interest in conductive polymers with a π-conjugated system (Azak, Kurbanoglu, Yildiz, & Ozkan, 2016; Çevik, Carbas, et al., 2018; M. Dervisevic, Dervisevic, et al., 2016). The term DTP, which is used to designate contiguous ring systems is composed of two thiophene rings attached to the pyrrole ring. Compounds with π-conjugation systems have been reported in many investigations due to their high conductivity and biocompatibility in field-effect transistors, optical devices, photovoltaic devices (Çevik, Carbas, et al., 2018), biosensors (Çevik, Carbas, et al., 2018; Dervisevic Cevik, et al. (2016); Parameswaran et al., 2009; Rasmussen & Evenson, 2013).

Herein, the electrochemical communication of *Leptolyngbia* sp. (CYN82) were accomplished using two different DTP type conducting polymers 4-(4H-dithieno[3,2-b:2′,3′-d]pyrrole-4-yl)aniline, P(DtP-Py-NH_2) and 5-(4H-dithieno[3,2-b:2′,3′-d]pyrol-4-yl) naphtalene-1-amine, P(DtP-Nptyl-NH_2) via electropolymerization. After that, p-aminothiophenol and 2-mercaptoethane functionalized gold nanoparticles (AuNPs) were cross-linked to the DtP polymers modified GE as a result of electropolymerization. Bioelectrodes were obtained by attaching of *Leptolyngbia* sp. onto the conducting polymer/AuNP modified GEs and stabilized on the electrode surface by using a dialysis membrane. These electrode structures generated an enhanced photocurrent due to high wiring capacity and high ET ability. Electrons formed as a result of oxidation in CYN82 by photosynthesis in water under visible light are easily transferred to the GE by DtP/AuNP structure. Bioelectrodes P(DtP-Py-NH_2)/AuNP/CYN82 and P(DtP-Nptyl-NH_2)/AuNP/CYN82 were tested with diuron, chlorpyrifos, and atrazine, which are important pesticides as seen by the decrease in photocurrent, which resulted from inhibition of photosynthesis by the pesticides.

2 | MATERIALS AND METHODS

2.1 | Materials

The chemical synthesis of two monomers was performed according to a previous report (Udum et al., 2014) and important explanations were added to the supplementary (5-(4H-dithieno[3,2-b:2′,3′-d]pyrol-4-yl) naphtalene-1-amine and 4-(4H-dithieno[3,2-b:2′,3′-d]pyrol-4-yl) aniline; Supporting Information Figures S1–S3). Cyanobacterium *Leptolyngbia* sp. (CYN82) was obtained from the Cawthron Institute Collection Culture of Microalgae, Nelson, New Zealand. Dialysis membrane (6,000–8,000 Da) was obtained from Spectra/Por Membrane Dialysis Products, Houston, dichloromethane (DCM), acetonitrile (ACN), $HAuCl_4$, 2-mercaptoethane sulfonic acid (MSA), ethanol, p-aminothiophenol (pAT), $FeCl_3.6H_2O$, $NaNO_3$, Na_2MoO_4 $2H_2O$, $NaHCO_3$, $CoCl_2.6H_2O$, $MgSO_4.7H_2O$, $MnCl_2.4H_2O$, $CaCl_2.2H_2O$, H_2SeO_3, K_2HPO_4, NaEDTA, H_3BO_3, $CuSO_4.5H_2O$, $ZnSO_4.7H_2O$,

vitamin B_{12}, biotin, phenyl-p-benzoquinon (PBQ), and thiamine HCl were supplied from Merck (Darmstadt, Germany). All other chemicals used in this study were supplied from Sigma-Aldrich (Munich, Germany), Merck and used as purchased without any extra purification. During this study ultra-pure water was used from Millipore Sigma (Milli-Q), Darmstadt, Germany source.

2.2 | Methods

2.2.1 | CYN82 growth condition and inoculum preparation

The cyanobacterial strains were collected from the New Zealand, Cawthron Institute Collection Culture of Microalgae, and photoheterotrophic growth experiments were done by taking aliquots of 4–5 mg wet masses of photoheterotrophically grown samples (which were collected at different times) added to 100 ml clear polystyrene bottles (Isolab, Istanbul, Turkey) containing 60 ml of MLA medium (Christopher & Bolch, 1996). MLA medium was used as growth medium and the cultivation procedure was performed at 22 ± 2°C under a white fluorescent light (10 W/m^2) source in a 12-hr light and 12-hr dark cycle under sterile conditions. To estimate the increase of mass each of the bottles were weighed once before adding the algae and reweighed after totally dried CYN82 was obtained. Ten bottles were set up and harvested once every 20 days because the optimum number of days for CYN82 to give the highest photocurrent response was obtained by time-dependent measurements between 5 and 30 days (data not shown). To harvest CYN82, a 20 ml cell suspension was collected, centrifuged (4,000 rpm) for 10 min at 20°C, and then the cell suspension was washed using MLA medium and centrifuged again under the same conditions.

2.2.2 | Synthesis of functionalized AuNP

AuNP functionalization was carried out by mixing of 190 mg of $HAuCl_4$, 42 mg of mercaptoethane sulfonate in 10 ml of ethanol solution, and 8 mg of p-aminothiophenol in 5 ml of methanol solution. The solution was then stirred for 1 hr in an ice bath while 2.5 ml of glacial acetic acid was added. After this procedure, this mixture was slowly mixed with 7.5 ml 0.1 M $NaBH_4$ solution until a dark solution was obtained. The resulting mixture was stirred overnight at room temperature, after which it was washed with methanol and diethyl ether. Characterization of MSA and pAT modified AuNP (with a diameter of 8 nm) has been reported in our previous study (Udum et al., 2014).

2.2.3 | Fabrication of bioelectrodes

Gold electrodes (GE) were cleaned using 65% sulfuric acid and 35% hydrogen peroxide solution (piranha solution) for a minute before any modification steps. Then, electrodes washed with Milli-Q water and then were left in an ultrasonic bath for 15 min in ethanol. Electropolymerization steps for the DtP-Py-NH_2 and DtP-Nptyl-NH_2 monomers were then carried out in the presence of a 0.1 M $TBAPF_6$/DCM/ACN (1:1:1) medium, at a potential range of 0.0 to 1.2 V and −1.0 to 1.0 V at a scan rate of 100 mV/s, respectively. After the electrode surfaces were coated with conducting polymers, functionalized AuNP (at different ratios) were added to the reaction cell. Binding of AuNP to the P(DtP-Py-NH_2) and P(DtP-Nptyl-NH_2) modified GE surfaces with polymeric oligoaniline bridges was obtained by cyclic voltammetry (CV) at potential ranges of 0 to 1.2 V and −1.0 to 1.0 V, respectively, in 50 mM, pH 7.4 phosphate buffer at a scan rate of 100 mV/s. The immobilization of the AuNPs, solutions including different amount of AuNP: 2, 1.5, 1, 0.5, 0.25, and 0.1% (in 50 mM, pH 7.4 sodium phosphate buffer [PBS]) and glutaraldehyde solution (1.0% in 50 mM, pH 7.4 PBS) were spread onto the modified GE. Then, the electrodes were incubated under sterile conditions at room temperature for 60 min. Dropwise addition of CYN82 which has a certain concentration (mg/ml) was used on the surface of the GE/polymer/AuNP electrode. A dialysis membrane was used to hold the CYN82 firmly on the surface of the modified P(DtP-Py-NH_2)/AuNP and P(DtP-Nptyl-NH_2)/AuNP GEs. As shown in Scheme 1, a dialysis membrane which was stored in PBS, was cut to cover the electrode surface and it was attached to the electrode surface with an O-ring for fixing of CYN82 on the surface of the GE/Polymer/AuNP electrode. In the last step, the edges of the dialysis membrane were wrapped using para film to obtain a solid structure.

2.2.4 | Photocurrent generation experiments and experimental variables

In this study, all photocurrent measurements were made using a special light simulator. The light source produces 1,300 W of light

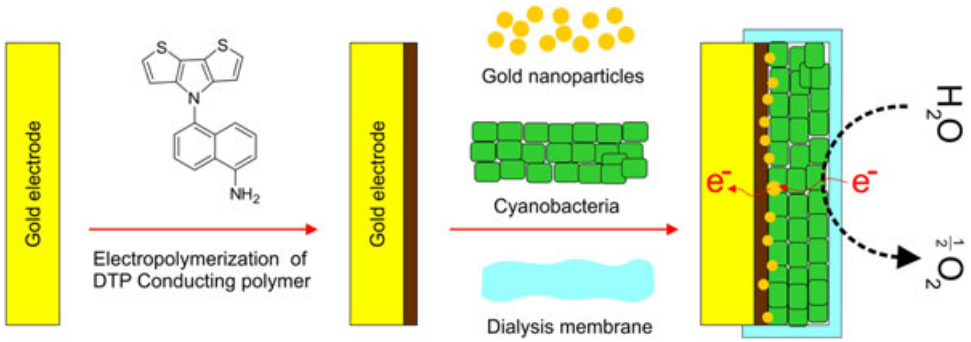

SCHEME 1 Schematic representation of GE/P(DtP-Nptyl-NH_2)/AuNP/CYN82 type bioelectrode fabrication [Color figure can be viewed at wileyonlinelibrary.com]

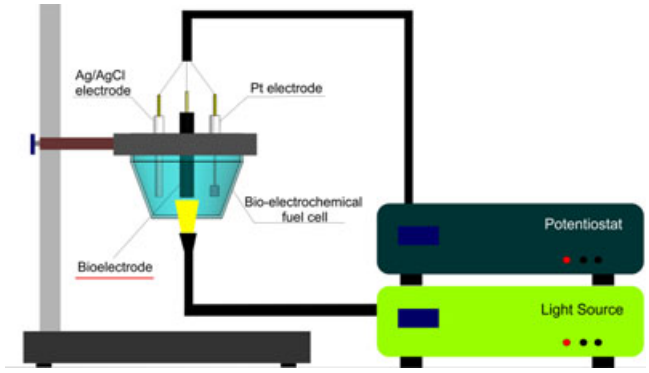

SCHEME 2 Schematic representation of BFC and experimental setup [Color figure can be viewed at wileyonlinelibrary.com]

with a photochemical Xenon lamp (Oriel, Model 6258, London, UK) has a 2 nm resolution and can transfer the light produced by fiber optic cable to the desired location. The translation of electrical data coming from the cell into digital data was performed by a phase-sensitive detector (Stanford Research Model SR 830 DSP, Sunnyvale, CA). For all photocurrent experiments (chronoamperometry [CA], constant potential), a three-electrode cell configuration was used in the 50 mM, pH 7.4 PBS and 1,300 W/m^2 visible range light was applied to the system (Scheme 2). Bioelectrodes (diameter of 3 mm) modified with P(DtP-Py-NH$_2$)/AuNP/CYN82 and P(DtP-Nptyl-NH$_2$)/AuNP/CYN82 were placed in the cell between a Pt foil electrode, which served as the cathode versus a saturated Ag/AgCl electrode. This system was connected to a Potentiostat/galvanostat (EG&G Model 263, IL) to perform CA and CV measurements. The cyclic on-off illumination CA measurements were evaluated ~50 s on and ~50 s off depending on the BFC reaching the pseudo-steady-state (Çevik, Carbas, et al., 2018), if not stated otherwise. All CA measurements were performed by applying a stable stirring (750 rpm) to the photo-bioelectrochemical fuel cell to achieve the maximum photocurrent density by increasing the electron diffusion rate. Before the experiments, argon gas was passed through the system for 15 min. Applied potential studies were performed by using different bioelectrodes and 0 V was selected as the optimum applied potential for all photocurrent measurements (Supporting Information Figure S4). All experimental variables were determined by using a constant 0 V versus Ag/AgCl, and 50 mg/ml CYN82.

The three-electrode cell configuration was used for all cyclic voltammetry experiments and a scan rate of 100 mV/s (unless otherwise stated) was applied for regular measurements. These measurements were performed at a constant potential (0 V) applied against Ag/AgCl in 50 mM, pH 7.4 PBS. All CV measurements were performed at 22 ± 2°C. All of the data expressed here are obtained from three different experiments and shows the average value.

3 | RESULTS AND DISCUSSION

3.1 | Possible electricity production mechanisms

The presumed ET by the action of conducting polymers, AuNPs, and the mediator is shown in Scheme 3 from random CYN82 to the electrode. The schematic of extracellular ET (EET) from photoheterotrophically grown CYN82 begins with photo-oxidation of water when the PSII gets excited by light (photon). ET continues through a group of electron carrier quinone complexes (Q_A and Q_B). The

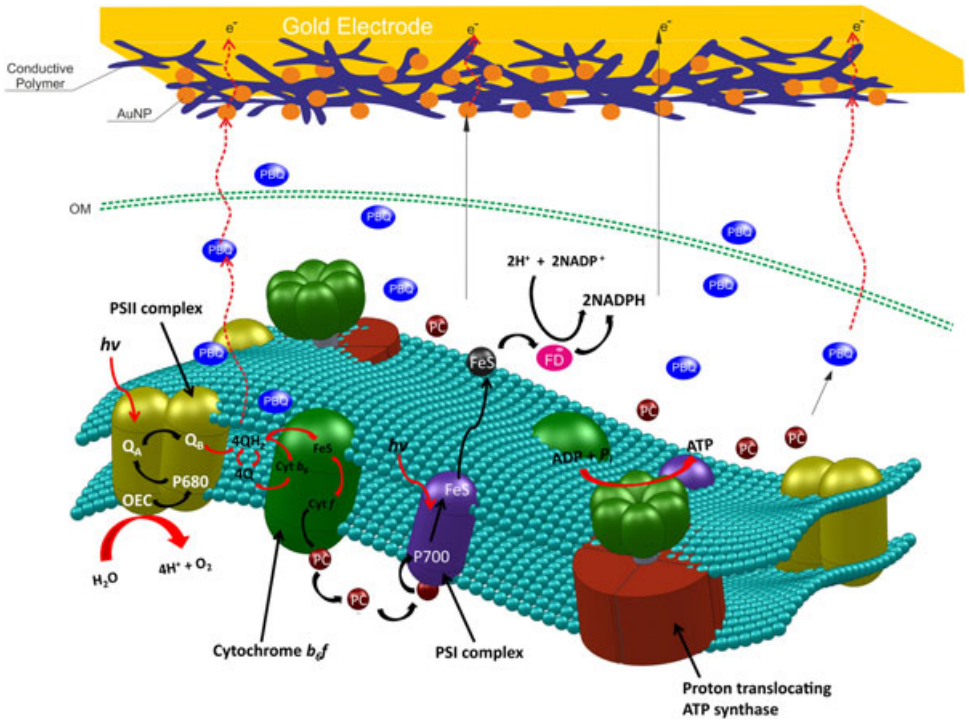

SCHEME 3 Schematic representation of light dependent possible electron transfer pathways from the reaction center to the electrode [Color figure can be viewed at wileyonlinelibrary.com]

reaction is followed by further ET to Cyt b_6f inside the cytochrome by a quinone cycle as illustrated in Scheme 3. Inside the membrane plastocynine is assumed to oxidize and carry electrons to the PSI. Further reactions generate a proton flow across the membrane and results in ATP formation. Here, ET can be described in several possible ways from the cell membranes of the cyanobacteria to the surface of the electrode (Çevik, Titiz, & Şenel, 2018).

The first ET pathway is a direct elecron transfer exhibited in Scheme 3. ET starts from the PSII then follows the route quinone pool (Q_A and Q_B)–PBQ–electrode, respectively. Polymers are typical mediators, which can make close interaction with cyanobacteria and molecularly contact with the outer membrane. The redox active site of the polymers enables the ET to the electrode (Çevik, Bahar, Şenel, & Abasıyanık, 2016). The ET from a possible oxidation reduction mechanism is another possible pathway. Photons absorbed by PSI (P700 complex) and followed by an emission of electron to a carrying molecule called iron sulphur (FeS) then transfer to the FD, which plays important role in the oxidation reduction process of $NADP^+$ to NADPH. Electron capture might be possible by polymer/AuNP passing through the pores in the outer membrane, then reacting with these charged molecules via the transmembrane proteins located in the cytoplasm membrane.

3.2 | Determination of experimental variables

Electropolymerization of the (DtP-Py-NH_2) monomer, was evaluated on a GE in 0.1 M $TBAPF_6$/DCM/ACN (1:1:1) medium at a scan rate of 100 mV/s. A wide oxidation peak of the monomer was determined around 0.8 V in the forward scan and a reduction peak was observed around 0.3 V (Ag/AgCl reference electrode). A conducting polymer film was successfully deposited on the GE as seen in the cyclic voltammogram and broad oxidation and reduction peaks were clearly observed. The increase in peak intensities obtained at repeated cycles showed that the polymer film thickness deposited on the electrode surface was a controlled process (Figure 1a).

The cyclic voltammetry of MSA and pAT functionalized AuNP attached to the P(DtP-Py-NH_2) polymer coated GE in a potential range of 0.0 to 1.2 V in 50 mM, pH 7.4 PBS at a scan rate of 100 mV/s (Figure 1b). The cross-linking established between modified AuNP and the P(DtP-Py-NH_2) modified electrode was affected the characteristic peaks and intensities of the polymer observed in the voltammogram (Azak et al., 2016; Udum et al., 2014). This can be explained by the high electron conducting property of the AuNP well immobilized and penetrating into the polymer structure.

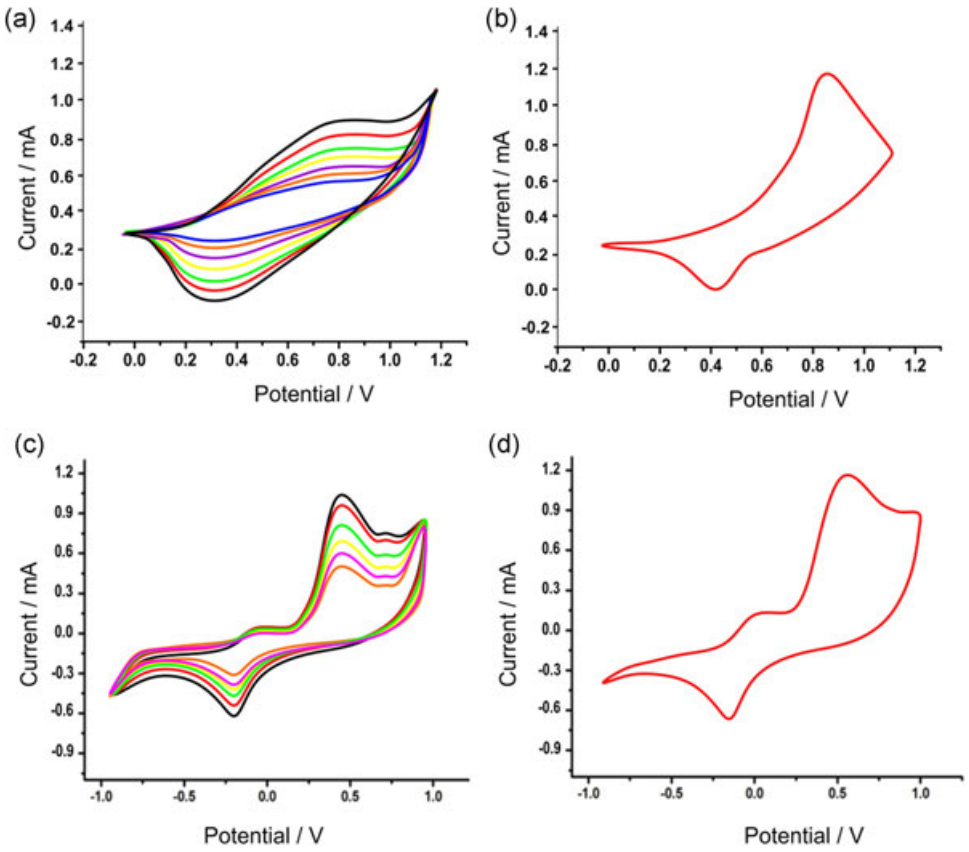

FIGURE 1 (a) Electropolymerization of DtP-Py-NH_2 monomer in 0.1 M $TBAPF_6$:DCM:CAN solvent–electrolyte at a scan rate of 100 mV/s. (b) CV of P(DtP-Py-NH_2)/AuNP structure in 50 mM, pH 7.4 PBS at a scan rate of 100 mV/s. (c) Electropolymerization of the DtP-Nptyl-NH_2 monomer in 0.1 M $TBAPF_6$:DCM:ACN solvent–electrolyte at a scan rate of 100 mV/s. (d) CV of P(DtP-Nptyl-NH_2)/AuNP structure in 50 mM, pH 7.4 PBS at a scan rate of 100 mV/s. AuNP: gold nanoparticles; DTP: alkoxy-bridged dithieno(3, 2-B:2′,3′-D) pyrrole; CV: cyclic voltammetry; PBS: sodium phosphate buffer. P(DtP-Nptyl-NH2): 5-(4H-dithieno [3,2-b:2,'3'-d]pyrol-4-yl) naphtalene-1-amine; P(DtP-Py-NH2): 4-(4H-Dithieno [3,2-b:2,'3'-d]pyrrole-4-yl)aniline [Color figure can be viewed at wileyonlinelibrary.com]

For the construction of the P(DtP-Nptyl-NH_2)/AuNP electrode, first of all electropolymerization of DtP-Nptyl-NH_2 monomer was evaluated on the bare GE by using CV between −1.0 and 1.0 V in 0.1 M $TBAPF_6$/DCM/CAN (1:1:1) medium at a scan rate of 100 mV/s (Figure 1c). Characteristic peaks of the P(DtP-Nptyl-NH_2) were observed around 0.5 (oxidation) and −0.4 V (reduction) in the voltammogram. Immobilization of the MSA and pAT modified AuNPs onto the P(DtP-Py-NH_2) coated GE were obtained by using a glutaraldehyde cross-linker. The obtained electrodes were characterized by using CV in a potential range of −1.0 to 1.0 V in 50 mM, pH 7.4 PBS at a scan rate of 100 mV/s (Figure 1d). The oxidation and the reduction peaks shifted to more positive and a change of peak intensities were observed. These attributed to the change in the polymer structure by the effect of AuNP immobilization.

Cyclic voltammetry studies were performed to express the redox activity of GE/P(DtP-Ph-NH_2) and CYN82 cell modified GE/P(DtP-Ph-NH_2)/CYN82 electrodes in the range of 0.0 to 1.2 V upon a cyclic on-off illumination of light (1,300 W/cm^2). Supplementary Information Figure S5a shows that no peak was obtained from the GE/P(DtP-Ph-NH_2) and no considerable change was observed whether under the light off (exhibited as black line) and light on (exhibited as blue line) conditions. When the electrode was modified with CYN82 a decrease was observed in the anodic (Ipc) and cathodic (Ipa) peak currents (exhibited as red line) under the light off condition. A considerable current change was observed under the light on condition (exhibited as green line). Supplementary Information Figure S5b shows the cyclic voltammogram of GE/P(DtP-Naptyl-NH_2) and GE/P(DtP-Nptyl-NH_2)/CYN82 upon cyclic on-off illumination in the range −1.0 V to 1.0 V. Good redox peaks were observed from the P(DtP-Nptyl-NH_2) modified electrode (black line) and formal potentials (E^0) for the Ipc and Ipa were recorded −0.1 and 0.5 V, respectively. After 50 mg/ml CYN82 was spread on top of the electrode, it is clearly seen from the figure, the current intensity was dramatically decreased (red line, light off condition). When the electrode was illuminated a considerable current difference was observed on the cyclic voltammogram (green line). The result suggests that the both polymers act as a wire to connect cyanobacteria and GE to carry electrons using possible routes.

Various control experiments have been carried out to demonstrate how to generate a photocurrent when the CYN82 was immobilized on the bare (without any modification) and polymer coated GE. The GE/CYN82 electrode (50 mM, pH 7.4 PBS) was illuminated by a light source having an intensity of 1,300 W/m^2 and it was observed that it could not produce a significant photocurrent

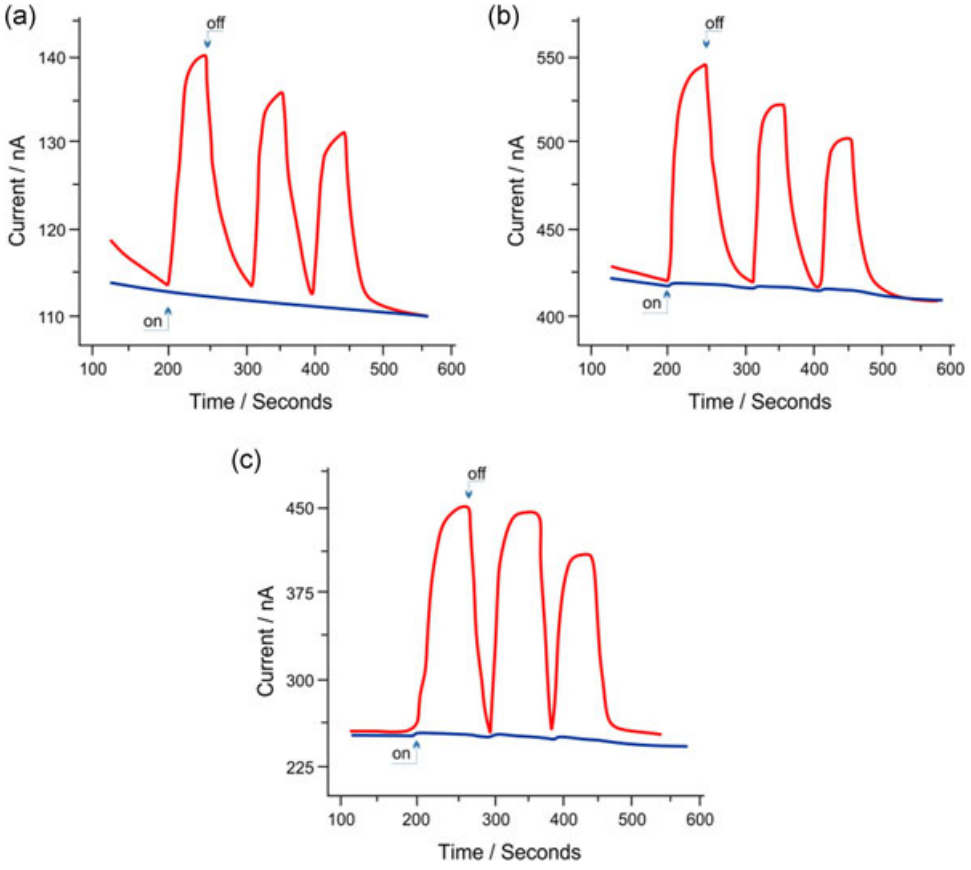

FIGURE 2 (a) The CA of a CYN82 modified GE in 50 mM, pH 7.4 PBS (blue line) and CA of a CYN82 modified GE in 50 mM, pH 7.4 PBS containing 0.410 μmol phenyl-p-benzoquinon (red line). (b) The CA of GE/P(DtP-Py-NH_2)/CYN82 (red line) and GE/ P(DtP-Py-NH_2) (blue line) in 50 mM, pH 7.4 PBS. (c) The CA of GE/P(DtP-Nptyl-NH_2)/CYN82 (red line) and GE/P(DtP-Nptyl-NH_2; blue line) in 50 mM, pH 7.4 PBS. The CA experiments were obtained under on off illumination of light at an intensity of 1,300 W/m^2, applied potential; 0 V (vs. Ag/AgCl). CA: chronoamperometry; GE: gold electrodes; PBS: sodium phosphate buffer; P(DtP-Nptyl-NH2): 5-(4H-dithieno [3,2-b:2,'3'-d]pyrol-4-yl) naphtalene-1-amine; P(DtP-Py-NH2): 4-(4H-Dithieno[3,2-b:2,'3'-d]pyrrole-4-yl)aniline [Color figure can be viewed at wileyonlinelibrary.com]

density (Figure 2a blue line). However, when a freshly prepared bare GE/CYN82 was illuminated by the same light intensity in 50 mM, pH 7.4 PBS containing 0.410 μmol phenyl-p-benzoquinon, a 25 nA photocurrent formation was observed (Figure 2a red line). From these results, it can be understood that a mediator in the solution or a special structure that is built on GE should be needed to accelerate the transfer of electrons formed from water oxidation through photosynthesis to the electrode and as a result be able to get photocurrent.

After the GEs had been coated with P(DtP-Py-NH_2) and P(DtP-Nptyl-NH_2) by using electropolymerization for 40 cycles for both systems and 50 mg/ml CYN82 was attached on the polymer coated surface. After that, electrodes were immersed in 50 mM, pH 7.4 PBS and the systems were illuminated with 1,300 W/m^2 visible light under 0 V constant potential. The values of photocurrents obtained increased (red lines) up to 125 and 195 nA for GE/P(DtP-Py-NH_2)/CYN82 and GE/P(DtP-Nptyl-NH_2)/CYN82, respectively (Figure 2b,c). The CA of the GE/Polymers is shown in blue lines (without CYN82) upon a cyclic on-off illumination of 1,300 W/m^2 and no photocurrent formation was observed. This showed that the enhancement of ET and wiring of more CYN82 to the electrode was achieved by the P(DtP-Py-NH_2) and P(DtP-Nptyl-NH_2) polymers. Bioelectrochemical systems GE/P(DtP-Py-NH_2)/CYN82 and GE/P(DtP-Nptyl-NH_2)/CYN82 that were prepared under the same conditions were tested with an ethanol solution instead of water, and treated with 1,300 W/m^2 of light in the visible range. After these tests, it was seen that there had not been any observation of photocurrent generation (data not shown). According to the results of the tests, this study shows that the BFC structure is only sensitive to water and shows that photocurrent is produced by ET as a consequence of water oxidation, which is caused by photosynthesis with light.

Polymers P(DtP-Py-NH_2) and P(DtP-Nptyl-NH_2) were coated on the GE surface using different numbers of voltammetry cycles to obtain the maximum photocurrent from the bioelectrodes. Polymers with different thicknesses were deposited on the working electrodes with 20, 40, 60, 80, and 100 cycles to find the optimum thickness. The thickness can be measured in terms of the charge passing through the cell. The film thicknesses for 20, 40, 60, 80, and 100 cycles polymer films of P(DtP-Py-NH_2) and P(DtP-Nptyl-NH_2) were calculated as 17 and 24 nm for 20 cycles, 32 and 41 nm for 40 cycles, 48 and 66 nm for 60 cycles, 61 and 82 nm for 80 cycles, and 86 and 107 nm for 100 cycles, respectively. A photocurrent value of 285 and 346 nA was clearly observed from the P(DtP-Py-NH_2) with 60 cycles (Figure 3a) and P(DtP-Nptyl-NH_2) with 40 cycles (Figure 3b),

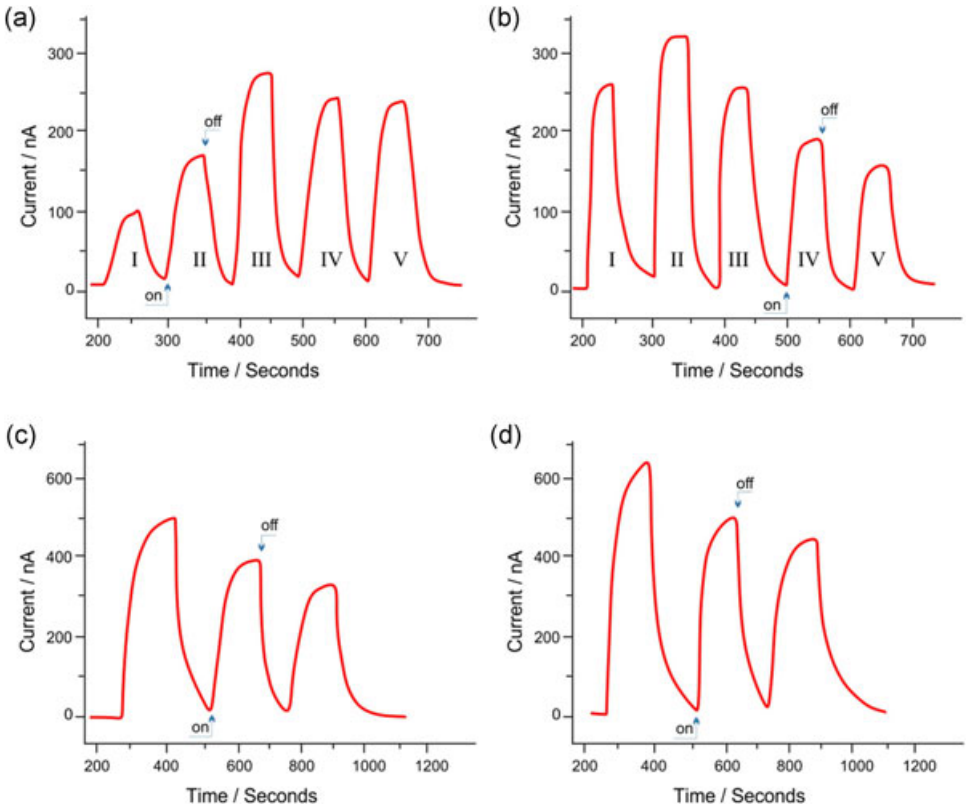

FIGURE 3 CAs of CYN82 modified (a) GE/P(DtP-Py-NH_2), and (b) GE/P(DtP-Nptyl-NH_2) electrodes with different cyclic voltammetry cycles: (I) 20, (II) 40, (III) 60, (IV) 80, and (V) 100 applied for P(DtP-Py-NH_2) and P(DtP-Nptyl-NH_2) polymer coating. (c) CA of AuNP immobilized P(DtP-Py-NH_2)/AuNP/CYN82 bioelectrode. (d) CA of AuNP immobilized P(DtP-Nptyl-NH_2)/AuNP/CYN82 bioelectrode. All CA measurements were obtained under on-off illumination of light at an intensity of 1,300 W/m^2, applied potential; 0 V (vs. Ag/AgCl). AuNP: gold nanoparticles; CA: chronoamperometry. GE: gold electrode; P(DtP-Nptyl-NH2): 5-(4H-dithieno [3,2-b:2,'3'-d]pyrol-4-yl) naphtalene-1-amine; P(DtP-Py-NH2): 4-(4H-Dithieno[3,2-b:2,'3'-d]pyrrole-4-yl)aniline [Color figure can be viewed at wileyonlinelibrary.com]

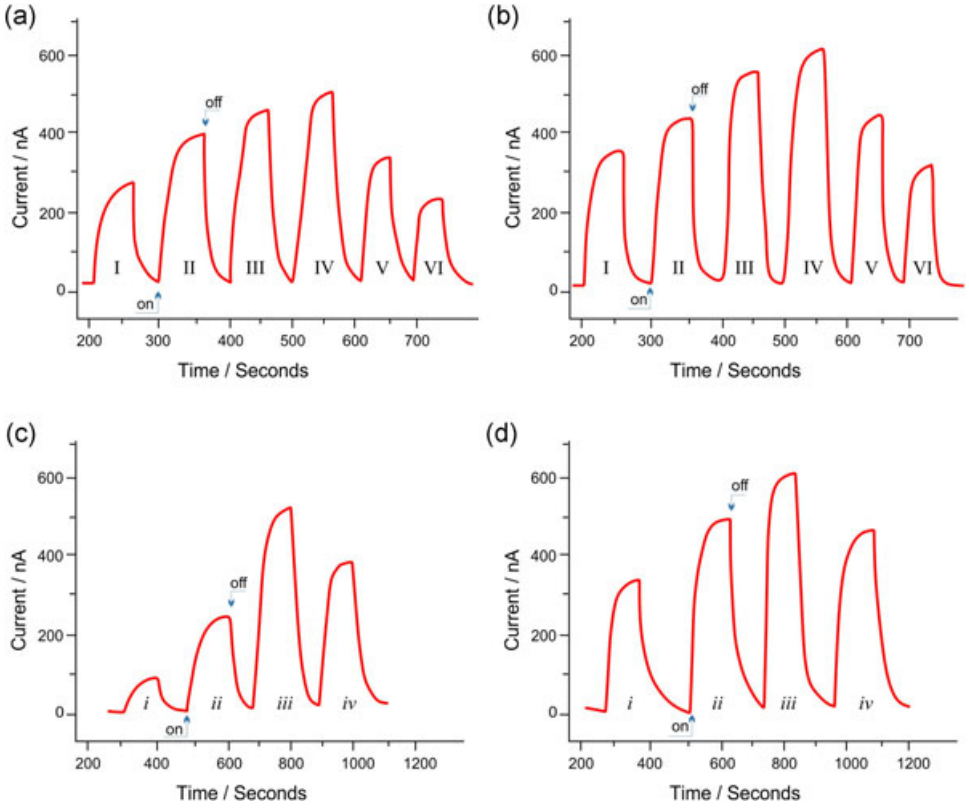

FIGURE 4 The photocurrent experiments of (a) GE/P(DtP-Nptyl-NH_2)/AuNP/CYN82. (b) GE/P(DtP-Py-NH_2)/AuNP/CYN82 bioelectrodes having different concentrations of AuNP; (I) 0.1%, (II) 0.25%, (III) 0.5%, (IV) 1%, (V) 1.5%, and (VI) 2% in 50 mM, pH 7.4 PBS under illumination at an intensity of 1,300 W/m^2, applied potential; 0 V (vs. Ag/AgCl). (b) The photocurrent experiments of (c) GE/P(DtP-Py-NH_2)/AuNP/CYN82. and (d) GE/P(DtP-Nptyl-NH_2)/AuNP/CYN82 bioelectrodes with different concentration of CYN82 (*i*) 25 mg/ml, (*ii*) 50 mg/ml, (*iii*) 75 mg/ml, and (*iv*) 100 mg/ml in 50 mM, pH 7.4 PBS under illumination at an intensity of 1,300 W/m^2, applied potential; 0 V (vs. Ag/AgCl). GE: gold electrode; P(DtP-Nptyl-NH2): 5-(4H-dithieno [3,2-b:2,'3'-d]pyrol-4-yl) naphtalene-1-amine; P(DtP-Py-NH2): 4-(4H-Dithieno[3,2-b:2,'3'-d]pyrrole-4-yl)aniline [Color figure can be viewed at wileyonlinelibrary.com]

respectively. Further increases in the electropolymerization cycles caused a decrease in photocurrent values observed in both systems. This indicates that the polymer film thickness directly affects the ET rate and should be optimized. With the polymer coating cycles, higher than 60 and 40 for P(DtP-Py-NH_2) and P(DtP-Nptyl-NH_2), respectively, the conductive polymer films thicken and prevent ET so that the number of electrons reaching the electrode is reduced and the photocurrent is decreased. After that, to study the effect of AuNP on ET regular CA experiments were evaluated. AuNP 0.5% in wt/vol were immobilized to the GE modified with P(DtP-Py-NH_2) obtained 60 cycles. The construction of the bioelectrode was completed by immobilizing 50 mg/ml CYN82 onto the P(DtP-Py-NH_2)/AuNP modified GE. For the preparation of P(DtP-Nptyl-NH_2)/AuNP/CYN82 modified GE, the DtP-Nptyl-NH_2 monomer was electropolymerized on the bare GE using 40 cycles and then AuNP (0.5% in wt/vol) were bonded via glutaraldehyde. Construction of the bioelectrode was completed by immobilizing 50 mg/ml CYN82 onto the P(DtP-Nptyl-NH_2)/AuNP modified GE.

Figure 3c,d represents the use of AuNP, an electron carrier between the electrodes and CYN82. It increased the amount of photocurrent obtained up to 540 and 630 nA for P(DtP-Py-NH_2)/AuNP/CYN82 and P(DtP-Nptyl-NH_2)/AuNP/CYN82 modified GE, respectively. This result indicates the not all previously immobilized CYN82 are wired with the electrode before bonding of AuNP. The AuNP increase the amount of transferred electrons from CYN82 to the electrode.

The optimum amount of AuNP immobilized to the P(DtP-Py-NH_2) and P(DtP-Nptyl-NH_2) film was also done. For the immobilization of the AuNP, after coating the GEs with P(DtP-Py-NH_2) and P(DtP-Nptyl-NH_2) by using 60 and 40 electropolymerization cycles, respectively: 2, 1.5, 1, 0.5, 0,25, and 0.1% (wt/vol) of AuNP in 5.0 ml, 50 mM, pH 7.4 PBS and glutaraldehyde solution 1.0% in 50 mM, pH 7.4 PBS were spread over the polymer coated GEs. After modification of AuNP, P(DtP-Py-NH_2)/AuNP and P(DtP-Nptyl-NH_2)/AuNP structures were obtained and 50 mg/ml CYN82 was spread onto the surfaces. Figure 4a,b shows the CA measurement of the GE/P(DtP-Py-NH_2)/$AuNP_x$/CYN82 and GE/P(DtP-Nptyl-NH_2)/$AuNP_x$/CYN82 (X: 2, 1.5, 1, 0.5, 0,25, and 0.1% [wt/vol] of AuNP) in 50 mM, pH 7.4 PBS under on-off illumination at an intensity of 1,300 W/m^2, applied potential; 0 V (vs. Ag/AgCl). It was observed that as the concentration of AuNP bound to the polymer film increased, the amount of photocurrent in both systems increased. This uptrend continued to 0.5% of the AuNP concentration, and over

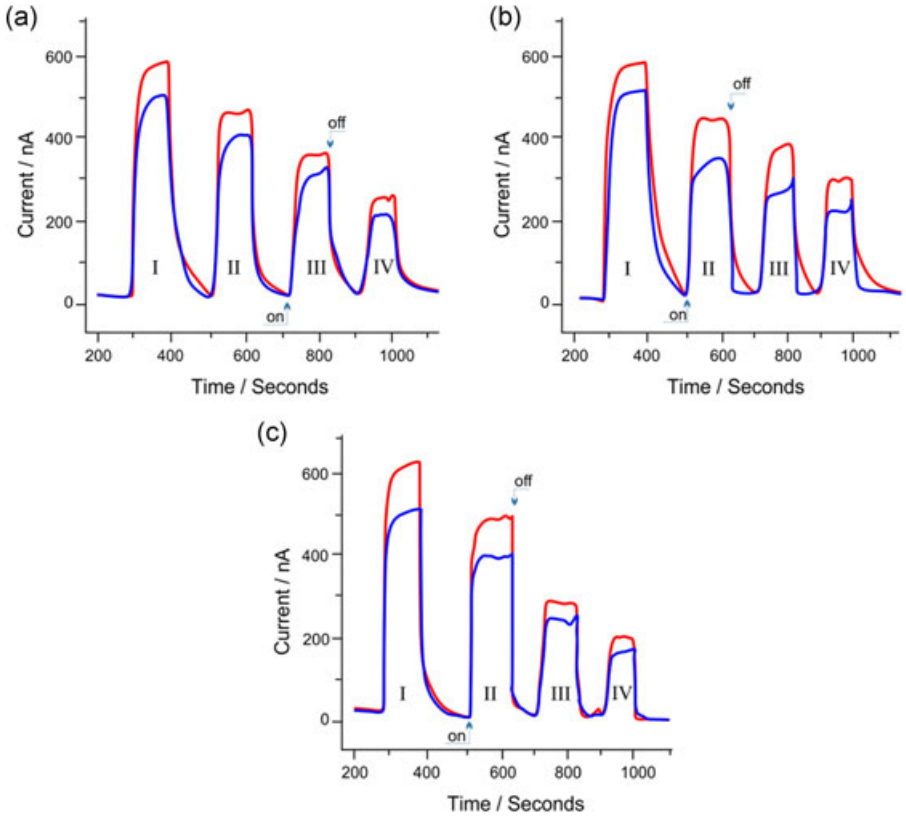

FIGURE 5 The photocurrent inhibition by specific inhibitors (a) diuron, (b) atrazine, and (c) chlorpyrifos tested with P(DtP-Py-NH_2)/AuNP/CYN82 and P(DtP-Nptyl-NH_2)/AuNP/CYN82 bioelectrodes shown in blue line and red line, respectively. The following concentrations were applied:(I) 0 mM to (II) 0.2 mM, (III) 0.3 mM, (IV) 0.5 mM. Regular chronoamperometry (CA) measurements were performed in 50 mM, pH 7.4 sodium phosphate buffer (PBS) under illumination at a light intensity of 1,300 W/m^2, applied potential; 0 V (vs. Ag/AgCl). P(DtP-Nptyl-NH2): 5-(4H-dithieno [3,2-b:2,'3'-d]pyrol-4-yl) naphtalene-1-amine; P(DtP-Py-NH2): 4-(4H-Dithieno[3,2-b:2,'3'-d]pyrrole-4-yl) aniline [Color figure can be viewed at wileyonlinelibrary.com]

0.5%, the increase in photocurrent continued to decrease. The increase of photocurrent up to 0.5% can be explained as the function of AuNP acting as an electron carrier between the electrode and CYN82. However, when the AuNP concentration was increased to 1% or more (1.5 and 2%), it was found that the photocurrent amount reached saturation or even began to decrease. This can be explained by the fact that the increase in AuNP concentration decreases the interaction with CYN82 cells by making a more rigid composite structure together with the polymer. Thus, it is thought that less CYN82 is in electrochemical communication with the electrode and this reduces the photocurrent.

Another characterization of P(DtP-Py-NH_2)/AuNP/CYN82 and P(DtP-Nptyl-NH_2)/AuNP/CYN82 modified GE is the study of the amount of CYN82 used in the bioelectrode fabrication. All photocurrent optimization experiments were performed with 50 mg/ml CYN82 modified electrodes and CAs experiments have been carried out up to now. In this study, GE was modified with P(DtP-Ph-NH_2)/AuNP and P(DtP-Nptyl-NH_2)/AuNP structures under optimum conditions (conditions for GE/P(DtP-Py-NH_2): 60 cycles, AuNP: 0.5% [wt/vol], and GE/P(DtP-Nptyl-NH_2): 40 cycles, AuNP: 0.5% [wt/vol]). The on-off illumination of light was evaluated ~100 s on and ~100 s off depending on the BFC reaching the pseudo-steady-state. The solutions containing 25, 50, 75, and 100 mg/ml of CYN82 were immobilized on the electrodes coated with P(DtP-Py-NH_2)/AuNP and P(DtP-Nptyl-NH_2)/AuNP. Figure 4c,4d shows the CA results for both bioelectrodes, an increase in photocurrent was observed up to a concentration of 75 mg/ml. It was observed that the photocurrent values decreased after 75 mg/ml. The reasons of the decrease in photocurrent by increasing CYN82 concentration can have two possible reasons. The first reason might be explained as limited access of light to the bioelectrode due to the very high concentration of CYN82. The second reason is that the thickened biocomponent on the electrode surface may block the ET towards the electrode generated as a result of water oxidation via photosynthesis. Thus, 75 mg/ml was determined as the optimum amount of CYN82 to be used for a bioelectrode in BFC construction.

The comparison of the analytical performances of GE/P(DtP-Py-NH_2)/AuNP/CYN82 and GE/P(DtP-Nptyl-NH_2)/AuNP/CYN82 systems with previously reported BFCs are listed in Supporting Information Table S1. The results show that both fuel cells produce considerably higher current densities (63 and 54 mA/m^2, respectively), compared to the relevant literature.

Organic pollutants, such as pesticides, have serious effects on the contamination of surface and ground waters (Giacomazzi & Cochet, 2004; Solomon et al., 1996). If these pesticides are exposed to a low amount of 1 ng/ml and prolonged exposure, the human endocrine system will be severely damaged and result in cancer (Dam, Seidler, & Slotkin, 2000). In addition, it has been reported that these pesticides have side effects such as growth problems and inhibition of the photosynthesis mechanism in plants. Diuron (Boger & Schlue, 1976; Hasan, Çevik, et al., 2015), Atrazine (El-Sheekh, Kotkat, & Hammouda, 1994), and Chlorpyrifos (Delorenzo, Scott, & Ross, 2001) are the most widely used pesticides and they inhibit the PSII activity in the CYN82. These pesticides bind to Q_A or Q_B, making the transfer of electrons from PSII to

plastoquinone ineffective. When these organic chemicals are connected with Q_B from two possible electron carriers, the ET is completely shut off, but if they bind with Q_A, the ET slows down and is not completely stopped (Hasan, Çevik, et al., 2015; Hirano, Satoh, & Katoh, 1980; Hsu et al., 1986). Figure 5 compares the photocurrent values obtained using pesticide inhibited and uninhibited bioelectrodes from BFCs. Regular CA experiments were performed with two different bioelectrodes GE/P(DtP-Py-NH_2)/AuNP/CYN82 (conditions for P(DtP-Py-NH_2): 60 cycles, AuNP: 0.5% [wt/vol] and CYN82: 50 mg/ml; shown in blue line) and P(DtP-Nptyl-NH_2)/AuNP/CYN82 (conditions for P(DtP-Nptyl-NH_2): 40 cycles, AuNP: 0.5% [wt/vol] CYN82: 50 mg/ml; shown in red line) with three different pesticides diuron (Figure 5a), atrazine (Figure 5 b) and chlorpyrifos (Figure 5c). The CA result of noninhibited bioelectrodes were represented with (I) in the figures. Three different concentrations were applied and represented in the figures as: II, 0.2 mM; III, 0.3 mM; IV, 0.5 mM. The photocurrent experiments were obtained in 50 mM, pH 7.4 PBS with different pesticide concentrations: II, 0.2 mM; III, 0.3 mM; IV, 0.5 mM) upon a cyclic on-off illumination at an intensity of 1,300 W/m^2, applied potential; 0 V (vs. Ag/AgCl). It is clearly seen from all the figures that the effects of the diuron, atrazine, and chlorpyrifos on the photosynthesis were very well observed by comparing the resulting photocurrents. The photocurrent generation of BFCs is decreased when the pesticide concentrations increase. Almost similar properties were observed in both systems and maximal activity loss (62%) was observed in the presence of 0.5 mM chlorpyrifos (IV) compared with that of the noninhibiting bioelectrode. Photocurrent production was not completely stopped when exposed to pesticides, but severe activity losses were observed in all CA experiments.

4 | CONCLUSIONS

In this study, BFCs with an enhanced photocurrent from a new bioelectrode system, depending on the fabrication of conductive polymers P(DtP-Py-NH_2) and P(DtP-Nptyl-NH_2) were demonstrated. In the electrode architecture layer by using the layer production method; the conducting polymer, AuNP, CYN82, and dialysis membrane and a stable structure were obtained. CV experiments were performed for electrode assembly and characterization of the system. One of the most important features of the system is that the materials used such as the polymer and AuNP can be easily monitored by CV during assembly of the electrode. Photocurrent experiments proved the transfer of electrons were achieved and the effect of P(DtP-Py-NH_2) and P(DtP-Nptyl-NH_2) polymers reveal that the photocurrent obtained from the electrode using the polymer is almost eightfold greater than the electrode without using polymer. This result indicates that the polymer is highly effective in ET. Another important point in obtaining the enhanced photocurrent is the use of AuNP in the electrode structure. The results clearly show that the photocurrent measured from the electrodes with AuNP is higher than that of the other electrodes (without AuNP). Conductivity of AuNP and oligoaniline bridges serves as a very suitable surface for fast ET from CYN82 to the GE. These systems demonstrate that achieving high efficiency of artificial fuel cells will be achieved through the use of good electrical communication and natural components. In addition, in such artificial BFC systems, the platform for light dependent photocurrent generation, well-organized electrodes produce high photo-bioelectrochemical activity. Finally, it was observed that these bioelectrodes can be used as pesticide biosensors by the decrease in photocurrent which resulted from inhibition of photosynthesis by pesticides.

ACKNOWLEDGEMENT

This study was supported by the "TUBITAK-BIDEB 2219 Postdoctoral Fellowship" by its contribution to Huseyin Bekir Yildiz over the completion of all research.

ORCID

Emre Cevik http://orcid.org/0000-0003-2075-7361

REFERENCES

Azak, H., Kurbanoglu, S., Yildiz, H. B., & Ozkan, S. A. (2016). Electrochemical glucose biosensing via new generation DTP type conducting polymers/gold nanoparticles/glucose oxidase modified electrodes. *Journal of Electroanalytical Chemistry*, *770*, 90–97.

Bidwell, R. G. S. (1957). Photosynthesis and metabolism of marine algae: I. Photosynthesis of two marine flagellates compared with chlorella. *Canadian Journal of Botany*, *35*(6), 945–950.

Boger, P., & Schlue, U. (1976). Long-term effects of herbicides on the photosynthetic apparatus I. Influence of diuron, triazines and pyridazinones. *Weed Research*, *16*(3), 149–154.

Bolch, C. J. S., & Blackburn, S. I. (1996). Isolation and purification of Australian isolates of the toxic cyanobacterium *Microcystis aeruginosa* Kfitz. *Journal of Applied Phycology*, *8*, 5–13.

Bombelli, P., Bradley, R. W., Scott, A. M., Philips, A. J., McCormick, A. J., Cruz, S. M., … Cameron, P. J. (2011). Quantitative analysis of the factors limiting solar power transduction by Synechocystis sp. PCC 6803 in biological photovoltaic devices. *Energy & Environmental Science*, *4*(11), 4690–4698.

Bullen, R. A., Arnot, T. C., Lakeman, J. B., & Walsh, F. C. (2006). Biofuel cells and their development. *Biosensors and Bioelectronics*, *21*(11), 2015–45.

Carpentier, R., Loranger, C., Chartrand, J., & Purcell, M. (1991). Photoelectrochemical cell containing chloroplast membranes as a biosensor for phytotoxicity measurement. *Analytica Chimica Acta*, *249*(1), 55–60.

Çevik, E., Bahar, Ö., Şenel, M., & Abasıyanık, M. F. (2016). Construction of novel electrochemical immunosensor for detection of prostate specific antigen using ferrocene-PAMAM dendrimers. *Biosensors and Bioelectronics*, *86*, 1074–1079.

Çevik, E., Carbas, B. B., Senel, M., & Yildiz, H. B. (2018). Construction of conducting polymer/cytochrome C/thylakoid membrane based photo-bioelectrochemical fuel cells generating high photocurrent via photosynthesis. *Biosensors and Bioelectronics*, *113*, 25–31.

Çevik, E., Titiz, M., & Şenel, M. (2018). Light-dependent photocurrent generation: Novel electrochemical communication between biofilm and electrode by ferrocene cored poly(amidoamine) dendrimers. *Electrochimica Acta*, *291*, 41–48.

Dam, K., Seidler, F. J., & Slotkin, T. A. (2000). Chlorpyrifos exposure during a critical neonatal period elicits gender-selective deficits in the development of coordination skills and locomotor activity. *Developmental Brain Research*, *121*(2), 179–187.

Delorenzo, M. E., Scott, G. I., & Ross, P. E. (2001). Toxicity of pesticides to aquatic microorganisms: A review. *Environmental Toxicology and Chemistry*, *20*(1), 84–98.

Dervisevic, M., Cevik, E., Şenel, M., Nergiz, C., & Abasiyanik, M. F. (2016). Amperometric cholesterol biosensor based on reconstituted cholesterol oxidase on boronic acid functional conducting polymers. *Journal of Electroanalytical Chemistry*, *776*, 18–24.

Dervisevic, M., Dervisevic, E., Azak, H., Çevik, E., Şenel, M., & Yildiz, H. B. (2016). Novel amperometric xanthine biosensor based on xanthine oxidase immobilized on electrochemically polymerized 10-[4H-dithieno(3,2-b:2′,3′-d)pyrrole-4-yl]decane-1-amine film. Sensors and Actuators B: Chemical 225:181-187. *Journal of Electroanalytical Chemistry*, *776*, 18–24.

El-Sheekh, M. M., Kotkat, H. M., & Hammouda, O. H. E. (1994). Effect of atrazine herbicide on growth, photosynthesis, protein synthesis, and fatty acid composition in the unicellular green alga *Chlorella kessleri*. *Ecotoxicology and Environmental Safety*, *29*(3), 349–358.

Gajda, I., Greenman, J., Melhuish, C., & Ieropoulos, I. (2013). Photosynthetic cathodes for microbial fuel cells. *International Journal of Hydrogen Energy*, *38*(26), 11559–11564.

Giacomazzi, S., & Cochet, N. (2004). Environmental impact of diuron transformation: A review. *Chemosphere*, *56*(11), 1021–1032.

Gorby, Y. A., Yanina, S., McLean, J. S., Rosso, K. M., Moyles, D., Dohnalkova, A., … Fredrickson, J. K. (2006). Electrically conductive bacterial nanowires produced by *Shewanella oneidensis* strain MR-1 and other microorganisms. *Proceedings of the National Academy of Sciences of the United States of America*, *103*(30), 11358–11363.

Haehnel, W. (1977). Electron transport between plastoquinone and chlorophyll A1 in chloroplasts. II. Reaction kinetics and the function of plastocyanin in situ. *Biochimica et Biophysica Acta (BBA) - Bioenergetics*, *459*, 418–441.

Hasan, K., Çevik, E., Sperling, E., Packer, M. A., Leech, D., & Gorton, L. (2015). Photoelectrochemical wiring of *Paulschulzia pseudovolvox* (algae) to osmium polymer modified electrodes for harnessing solar energy. *Advanced Energy Materials*, *5*(22

Hasan, K., Reddy, K. V. R., Eßmann, V., Górecki, K., Conghaile, P. Ó., Schuhmann, W., … Gorton, L. (2015). Electrochemical communication between electrodes and rhodobacter capsulatus grown in different metabolic modes. *Electroanalysis*, *27*(1), 118–127.

Heldt, H.-W., & Piechulla, B. (2011). The use of energy from sunlight by photosynthesis is the basis of life on earth. *Plant Biochemistry* (Please provide the Editors for Reference "Heldt and Piechulla, 2011". Fourth ed, 43–64). San Diego: Academic Press.

Hernandez, M. E., & Newman, D. K. (2001). Extracellular electron transfer. *Cellular and Molecular Life Science*, *58*, 1662–1671.

Hirano, M., Satoh, K., & Katoh, S. (1980). Plastoquinone as a common link between photosynthesis and respiration in a blue-green alga. *Photosynthesis Research*, *1*(3), 149–162.

Hsu, B. D., Lee, J. Y., & Pan, R. L. (1986). The two binding sites for DCMU in photosystem II. *Biochemical and Biophysical Research Communications*, *141*(2), 682–688.

Khan, R., Solanki, P. R., Kaushik, A., Singh, S. P., Ahmad, S., & Malhotra, B. D. (2008). Cholesterol biosensor based on electrochemically prepared polyaniline conducting polymer film in presence of a nonionic surfactant. *Journal of Polymer Research*, *16*(4), 363–373.

Logan, B. H., Hamelers, B., Rozendal, R., Schroder, U., Freguia, J., Alterman, P., Verstraete, W., & Rabaey, K. (2006). Microbial fuel cells methodology and technology. *Environmental Science and Technology*, *40*(17), 5181–5192.

McCormick, A. J., Bombelli, P., Scott, A. M., Philips, A. J., Smith, A. G., Fisher, A. C., & Howe, C. J. (2011). Photosynthetic biofilms in pure culture harness solar energy in a mediatorless bio-photovoltaic cell (BPV) system. *Energy & Environmental Science*, *Please provide page numbers in the reference "McCormick et al. 2011".4*, 11.

Nishio, K., Hashimoto, K., & Watanabe, K. (2013). Light/electricity conversion by defined cocultures of Chlamydomonas and Geobacter. *Journal of Bioscience and Bioengineering*, *115*(4), 412–417.

Rahman, M., Kumar, P., Park, D.-S., & Shim, Y.-B. (2008). Electrochemical sensors based on organic conjugated polymers. *Sensors*, *8*(1), 118–141.

Parameswaran, M., Balaji, G., Jin, T. M., Vijila, C., Vadukumpully, S., Furong, Z., & Valiyaveettil, S. (2009). Charge transport studies in fluorene – Dithieno[3,2-b:2′,3′-d]pyrrole oligomer using time-of-flight photoconductivity method. *Organic Electronics*, *10*(8), 1534–1540.

Rashid, N., Cui, Y.-F., Saif Ur Rehman, M., & Han, J.-I. (2013). Enhanced electricity generation by using algae biomass and activated sludge in microbial fuel cell. *Science of the Total Environment*, *456-457*, 91–94.

Rasmussen, S. C., & Evenson, S. J. (2013). Dithieno[3,2-b:2′,3′-d]pyrrole-based materials: Synthesis and application to organic electronics. *Progress in Polymer Science*, *38*(12), 1773–1804.

Sawa, M., Fantuzzi, A., Bombelli, P., Howe, C. J., Hellgardt, K., & Nixon, P. J. (2017). Electricity generation from digitally printed cyanobacteria. *Nature Communications*, *8*(1), 1327.

Şenel, M., Bozgeyik, I., Çevik, E., & Fatih Abasıyanık, M. (2011). A novel amperometric galactose biosensor based on galactose oxidase-poly (N-glycidylpyrrole-co-pyrrole). *Synthetic Metals*, *161*(5-6), 440–444.

Sekar, N., Umasankar, Y., & Ramasamy, R. P. (2014). Photocurrent generation by immobilized cyanobacteria via direct electron transport in photo-bioelectrochemical cells. *Physical Chemistry Chemical Physics*, *16*(17), 7862–7871.

Şenel, M., Çevik, E., & Abasıyanık, M. F. (2010). Amperometric hydrogen peroxide biosensor based on covalent immobilization of horseradish peroxidase on ferrocene containing polymeric mediator. *Sensors and Actuators B: Chemical*, *145*(1), 444–450.

Şenel, M., Nergiz, C., Dervisevic, M., & Çevik, E. (2013). Development of amperometric glucose biosensor based on reconstitution of glucose oxidase on polymeric 3-aminophenyl boronic acid monolayer. *Electroanalysis*, *25*(5), 1194–1200.

Solomon, K. R., Baker, D. B., Richards, R. P., Dixon, K. R., Klaine, S. J., La Point, T. W., … Williams, W. M. (1996). Ecological risk assessment of atrazine in North American surface waters. *Environmental Toxicology and Chemistry*, *15*(1), 31–76.

Soylemez, S., Udum, Y. A., Kesik, M., Gündoğdu Hızlıateş, C., Ergun, Y., & Toppare, L. (2015). Electrochemical and optical properties of a conducting polymer and its use in a novel biosensor for the detection of cholesterol. *Sensors and Actuators B: Chemical*, *212*, 425–433.

Strik, D. P. B. T. B., Terlouw, H., Hamelers, H. V. M., & Buisman, C. (2008). Renewable sustainable biocatalyzed electricity production in a photosynthetic algal microbial fuel cell (PAMFC). *Applied Microbiology and Biotechnology*, *81*(4), 659–668.

Torimura, M., Miki, A., Wadano, A., Kano, K., & Ikeda, T. (2001). Electrochemical investigation of cyanobacteria *Synechococcus* sp. PCC7942-catalyzed photoreduction of exogenous quinones and photoelectrochemical oxidation of water. *Journal of Electroanalytical Chemistry*, *496*(1), 21–28.

Udum, Y. A., Yıldız, H. B., Azak, H., Sahin, E., Talaz, O., Çırpan, A., & Toppare, L. (2014). Synthesis and spectroelectrochemistry of dithieno (3,2-b:2′,3′-d)pyrrole derivatives. *Journal of Applied Polymer Science*, *131*, 8676–8683.

Vidal, J. C., Garcia, E., & Castillo, J. R. (2002). Development of platinized and ferrocene-mediated cholesterol amperometric biosensor based on electropolymerization of polypyrrole in a flow system. *Analytical Science*, *18*, 537–541.

Wang, C., Dong, H., Hu, W., Liu, Y., & Zhu, D. (2012). Semiconducting pi-conjugated systems in field-effect transistors: A material odyssey of organic electronics. *Chemical Reviews*, *112*(4), 2208–2267.

SUPPORTING INFORMATION

Additional supporting information may be found online in the Supporting Information section at the end of the article.

How to cite this article: Cevik E, Buyukharman M, Yildiz HB. Construction of efficient bioelectrochemical devices: Improved electricity production from cyanobacteria (*Leptolyngbia* sp.) based on π-conjugated conducting polymer/gold nanoparticle composite interfaces. *Biotechnology and Bioengineering*. 2018;1–12. https://doi.org/10.1002/bit.26885